ACS Photonics

pubs.acs.org/journal/apchd5

Letter

Nonlinear Wavy Metasurfaces with Topological Defects for Manipulating Orbital Angular Momentum States

Yang Ming, Wang Zhang, Jie Tang, Xifeng Yang, Yu-shen Liu,* and Yan-qing Lu*

Cite This: *ACS Photonics* 2021, 8, 1896−1902

Read Online

ACCESS | Metrics & More | Article Recommendations

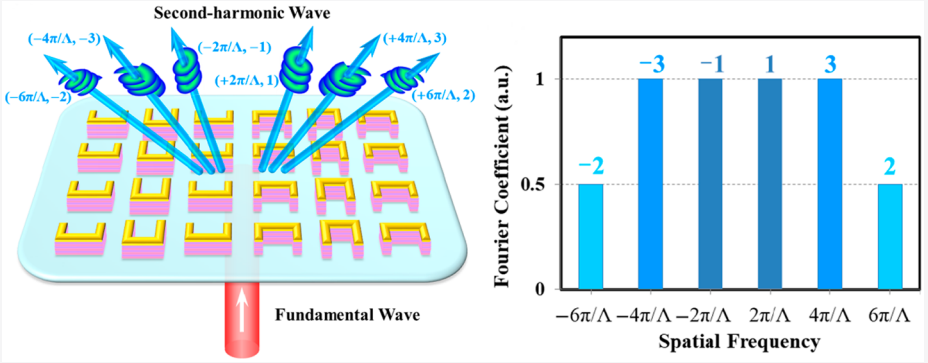

ABSTRACT: Patterned surfaces with rationally designed nanostructures provide a flexible platform for beam shaping in both the linear and nonlinear optical regime. The properties of reflected or diffracted output depend on the Fourier transform of the surface profile. To obtain ideal effects, the profile should contain a desired sum of specially formed sinusoidal terms with predefined superposition coefficients. Such a kind of surface is vividly described as a "wavy" surface in certain contexts, which has been widely utilized for linear optical applications. However, the nonlinear counterparts are rarely demonstrated. Here, we present a design framework of nonlinear "wavy" surfaces based on hybrid nanostructures of metal and multi-quantum-well (MQW) for generating and steering second-harmonic beams. Giant second-order nonlinearity is available in MQWs; thus, an efficient up-conversion process can be ensured. In this system, the harmonic output is determined by the Fourier spectrum of spatially dependent second-order nonlinearity, which can be engineered through tailoring the shape, orientation, and arrangement of nanoelements known as "meta-atoms". Compared with previously proposed nonlinear metasurfaces, the wavy design can be more flexible for manipulating orbital angular momentum (OAM) states through introducing topological defects. Besides choosing states with expected topological charges and controlling the relative weight, the rule in conventional binary $\chi^{(2)}$ systems that the attached OAM value increases with the order of reflection/diffraction can be broken via suitable nanostructure design, which means that lower order is possible to have larger absolute topological charge. This proposed framework has tremendous potential for applications in emerging areas such as quantum nanophotonics and topological photonics.

KEYWORDS: *nonlinear wavy metasurfaces, orbital angular momentum, multi-quantum-well*

The exploration of artificial materials has greatly changed the spirit of photonics and gives us the chance to become creative designers, enabling the modulation of the properties of light on demand. Among an enormous variety of artificial materials, nanopatterned interfaces are an attractive type that have aroused lively interest in the past decade.[1] The corresponding systems exhibit the unique abilities of controlling the amplitude,[2] phase,[3,4] and polarization[5,6] of a photon. For linear optical applications, various functional devices like phase-only transmissive spatial light modulator[7] and electromagnetically induced absorber[8] have been demonstrated based on metasurfaces with rationally designed nanostructures. Recently, as a further step, the potential of nanopatterned interfaces in the field of nonlinear optics draws considerable attention.[9−13] In early studies, nonlinear interactions at such interfaces always suffer from low conversion efficiency.[10,11] The exploitation of multi-quantum-wells (MQWs) with giant second-order nonlinearity for metasurfaces substantially eases the problem,[14−16] which paves the way for further development of this direction.

Received: March 3, 2021
Published: June 29, 2021

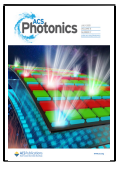

https://doi.org/10.1021/acsphotonics.1c00330
ACS Photonics 2021, 8, 1896−1902

Tailoring second-harmonic beams is always a crucial subject in nonlinear photonic applications, which is able to be realized through tuning the spatial profile of the second-order nonlinear coefficient $\chi^{(2)}$. Mathematically, the profile can be expressed as a Fourier sum of exponential functions, which are related to specified sinusoids. Theoretically, to obtain fine modulations, only desired sinusoids should be contained. In linear optical applications, two-dimensional interfaces with such features are vividly described as "wavy" surfaces in certain contexts.[17] The nonlinear counterparts of this kind of surface are rarely demonstrated, hence, we intend to explore this area. Here we still adopt the depiction "wavy", and that certainly does not correspond to the actual surface shape, but the distribution of $\chi^{(2)}$. For quasi-two-dimensional media formed by traditional ferroelectric dielectrics such as lithium niobate and potassium titanyl phosphate, the commonly used approach to tuning $\chi^{(2)}$ is domain engineering, which merely changes the sign between positive and negative, but not the modulus.[18−20] The modulation ability of these systems is limited to redistributing the weight of different Fourier terms, which is inadequate for complex tasks. In view of this situation, we present a design framework for more flexible beam shaping based on nonlinear metasurfaces consisting of hybrid meta-atoms of metal and MQW. In such a system, the effective nonlinear susceptibility is determined by the normal component of the local field.[14,15,21] Since it is influenced by the shape and orientation of meta-atoms, we can acquire a quasi-continuous variation of $\chi^{(2)}$ through tailoring the geometry and arrangement of them. This method will approach closer to ideal effects of Fourier-spectrum engineering along with the development of nanofabrication technologies. As a highly valuable degree of freedom for optical information processing,[22] the orbital angular momentum (OAM) of a photon keeps attracting lively research interest in recent years, which has been demonstrated to be effectively manipulated with liquid crystal devices,[23] chiral nanostructures,[24,25] and photonic crystals supporting bound states in the continuum.[26] Here we utilize the proposed wavy metasurfaces to steer OAM states through introducing topological defects. Compared with previously demonstrated nonlinear metasurfaces, the present ones are more powerful in this task. The reflection/diffraction can be flexibly controlled, and it is available to choose output OAM states with expected topological charges and regulate the relative weight. Moreover, if using the aforementioned conventional ferroelectric $\chi^{(2)}$ systems, the attached OAM value of output states increases with the order of reflection/diffraction.[18,27] However, this rule can be broken in the present system, and lower order makes it possible to have a larger absolute topological charge via a suitable nanostructure design. The detailed theories are constructed, and several one-dimensional examples are calculated for illustration. This potential platform could be further explored for valuable applications in quantum nanophotonics and topological photonics.

To clarify our design framework, the dynamics of nonlinear interactions at nanopatterned interfaces should be analyzed first. Three-wave mixing in nonlinear media is governed by the Helmholtz equation, including second-order polarization terms, which is usually reformulated as two coupled equations for describing second-harmonic generation[28]

$$\frac{\partial E_{2\omega}}{\partial z} = \frac{4i\omega^2}{k_{2\omega}c^2}\chi_{\text{eff}}E_{\omega}^2 e^{-i(k_{2\omega}-2k_{\omega})z}$$
$$\frac{\partial E_{\omega}}{\partial z} = \frac{i\omega^2}{k_{\omega}c^2}\chi_{\text{eff}}E_{\omega}^* E_{2\omega} e^{i(k_{2\omega}-2k_{\omega})z} \quad (1)$$

Here, the ω and k correspond to frequency and wave vector, respectively. E_{ω} and $E_{2\omega}$ are the fundamental and second-harmonic field envelopes. The effective nonlinear coefficient is χ_{eff}. It is a constant in traditional homogeneous nonlinear crystals. However, if we intend to tailor the second-harmonic beams to introduce OAM, a space-dependent $\chi^{(2)}$ is needed.

One of the most important characters of photon-carrying OAM is the helical phase $\exp(il\theta)$, and the parameter l is the topological charge, which can be any integer number, indicating that the photon possesses an OAM of $l\hbar$.[29] To modulate OAM states, the term $\exp(il\theta)$ should be appropriately integrated into $\chi^{(2)}(\vec{r})$ on demand according to the holographic principle,[18,19] and the corresponding expression is useful to be described in terms of a Fourier series as

$$\chi^{(2)}(\vec{r}) = \chi_0 \sum_{m,n} G_{m,n} e^{i(\vec{k}_m\cdot\vec{r}+l_n\theta)} \quad (2)$$

where $G_{m,n}$ and $e^{i(\vec{k}_m\cdot\vec{r}+l_n\theta)}$ are Fourier coefficient and basis, respectively. If the Fourier spectrum is not able to be finely engineered, the output is multi-order reflection or diffraction. Many unwanted orders are contained, and the generation efficiency of target order reduces. Through choosing a specified wavy variation for $\chi^{(2)}$, the exponential terms can be controlled, thus the desired output results are acquired including certain orders with predefined weight and OAM. In the simplest case with $\chi^{(2)}(x) = \chi_0\cdot\sin(2\pi x/\Lambda + \theta)$, we have $\chi^{(2)}(x) = \chi_0\cdot\sum_{\pm1}(m/2i)\exp[im(2\pi x/\Lambda + \theta)]$. The output is ±1 order with equal weight, and the corresponding topological charge is also ±1, respectively. If it is more complex, for $\chi^{(2)}(x) = (\chi_0/C_N)\cdot\sum_{n,k}F_{n,k}\sin(2\pi x/\Lambda_n + l_k\theta)$, the expansion is

$$\chi^{(2)}(x) = -\frac{\chi_0}{2C_N}\sum_{\substack{(n,k)\\(m=\pm1)}} imF_{n,k}\exp[im(2\pi x/\Lambda_n + l_k\theta)] \quad (3)$$

where n and k are two finite integers, and C_N is the normalized parameter which is equal to the maximum of $\sum_{n,k}F_{n,k}\sin(2\pi x/\Lambda_n + l_k\theta)$. Selecting appropriate $F_{n,k}$, Λ_n, and l_k, it is not hard to endow lower reflection/diffraction orders with larger OAM, and unwanted orders are eliminated.

Such variations of $\chi^{(2)}$ requires more complicated engineering of nanostructures. For nonlinear metasurfaces, this task can be realized based on the present nanofabrication technologies. The shape, orientation, and arrangement of meta-atoms are flexibly steered through technologies such as electron beam lithography and reactive ion etching.[9−12,30] They are all crucial influence factors of $\chi^{(2)}(\vec{r})$. A more complicated distribution of the second-order susceptibility can be realized through simultaneous controlling of these three factors. The local modulus mostly depends on the corresponding susceptibility tensor. According to nonlinear scattering theory,[9,11,14] the second-order nonlinear response of a meta-atom is quantified with the Lorentz reciprocity theorem as (more details can be found in the Methods section)

$$\chi_{ijk}^{(2)} = \chi_{nnn}^{(2)}\left[\int \xi_{in}(2\omega)\xi_{jn}(\omega)\xi_{kn}(\omega)\ \mathrm{d}V\right]/V \quad (4)$$

https://doi.org/10.1021/acsphotonics.1c00330
ACS Photonics 2021, 8, 1896−1902

where $\chi^{(2)}_{mn}$ is the nonlinear susceptibility decided by materials. The $\xi_{(j/k)n}$ and ξ_{in} represent the normalized field components on the normal direction to metasurface at the fundamental and second-harmonic frequencies, respectively. As an example, the case of nonlinear metasurfaces based on split ring resonators (SRRs) shown in Figure 1a is given. The geometry parameters

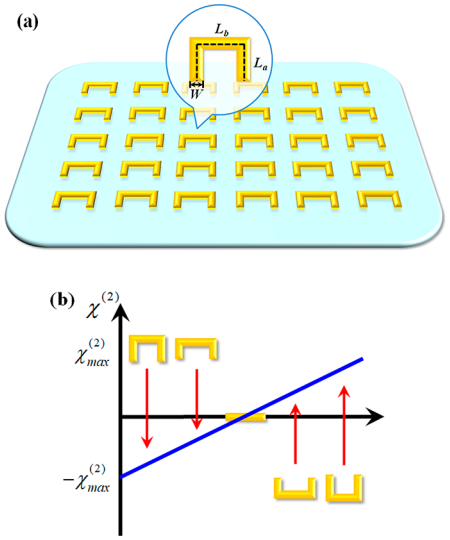

Figure 1. (a) Sketch of nonlinear metasurfaces consisting of SRRs, with the geometry parameters shown in the inset. (b) Value of $\chi^{(2)}$ varies with the shape and orientation of SRR meta-atom.

are defined in the inset, including L_a for the length of the arms, L_b for the length of the base, and W for the width. From Figure 1b, it can be seen that the absolute value of $\chi^{(2)}$ varies with the arm and base lengths L_a and L_b of meta-atom, and the sign of $\chi^{(2)}$ changes when the orientation of meta-atom is inverted.[13] Based on this approach, any wavy distribution of $\chi^{(2)}$ can be acquired through designing the nanostructures of nonlinear metasurfaces in theory. However, as the meta-atoms are discretized, the variation of $\chi^{(2)}$ is quasi-continuous. With the development in nanofabrication technologies, the spatial distribution density of meta-atoms could further increase, and the modulation of $\chi^{(2)}$ will approach closer to ideal effects.

Considering practical nonlinear metasurfaces, early studies focus on those based on pure metallic meta-atoms.[9−11] In such systems, the quadratic nonlinearity originates from microscopic symmetry break due to the geometry of meta-atoms. The local plasmonic resonance can bring enhancement for the nonlinear interactions, which makes the corresponding second-order susceptibility not smaller than those of common nonlinear optical crystals. The reported values are 10^1∼10^2 pm/V,[11,31] which are comparable with the d_{33} = 27 pm/V of $LiNbO_3$.[32] However, owing to the extremely short interaction length, that is not large enough. Later on, all-dielectric nonlinear metasurfaces are fabricated based on nonlinear materials such as AlGaAs.[33,34] The maximum of the corresponding $\chi^{(2)}$ is subject to component materials, and the value can hardly surpass the magnitude of 10^2 pm/V. The increase of nonlinear conversion efficiency is limited. Therefore, it is necessary to further seek for materials with much larger $\chi^{(2)}$. One of the most promising candidates is MQW. Intersubband transitions make MQW possess one of the largest known nonlinearities in condensed matter systems. The structures of MQW should be well-designed to support three electronic subbands, as is shown in Figure 2a. When the pump frequency is close to intersubband resonances, the second-order nonlinear susceptibility of MQW can be expressed as[14]

$$\chi^{(2)}_{nnn}(\omega) = N_e \frac{e^3}{\hbar^2 \varepsilon_0} \frac{z_{12} z_{23} z_{31}}{(\omega_{31} - 2\omega - i\gamma_{31})(\omega_{21} - \omega - i\gamma_{21})} \tag{5}$$

In the equation above, ω is the pump (fundamental) frequency, and ω_{ij} is the transition frequency between states i and j. For second-harmonic generation, ω_{32} is usually tuned to be equal to ω_{21}. The reduced Plank constant is signified by $\hbar$, and ε_0 is the vacuum permittivity. The parameter N_e represents the average carrier density, while e is the electron charge. Furthermore, ez_{ij} and γ_{ij} are the dipole moment and decay rate for the transition between i and j, respectively. Both of them are associated with the subband structures.

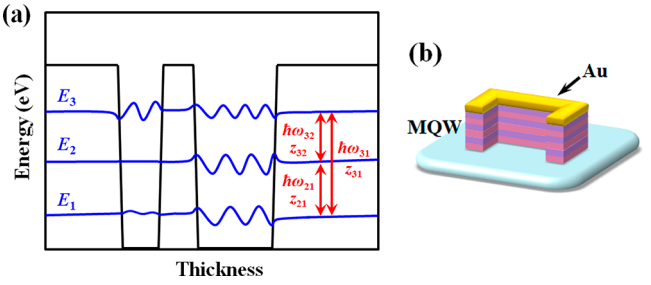

Figure 2. (a) General conduction band diagram of a quantum well structure. The three subbands are labeled with 1, 2, and 3. Transitions between subbands are represented by double-headed red arrows, and the transition energies and dipole moments are marked correspondingly. (b) Illustration of a hybrid meta-atom consisting of gold and MQW with SRR shape.

According to eq 5, there are two approaches to improving the second-order nonlinear coefficient $\chi^{(2)}$. If the product of dipole moments $e^3 z_{12} z_{23} z_{31}$ is extremely large, $\chi^{(2)}$ can be greatly enhanced. This effect is especially remarkable in asymmetric MQWs, such as InGaAs/AlInAs[14,21,35] and Ge/Si/SiGe[36] semiconductor heterostructures. The reported value of $\chi^{(2)}$ reaches 1.2 × 10^6 pm/V at high frequencies beyond mid-infrared region.[35] Moreover, $\chi^{(2)}$ can also be significantly increased when the pump frequency ω is in resonance with the transition frequency ω_{21} (ω_{32}). In coupled TiN/Al_2O_3 MQWs, besides the large dipole moment, such a peak of $\chi^{(2)}$ is available to be tuned to the visible/near-infrared (NIR) band owing to the extreme depth of structural units.[16] The value of $\chi^{(2)}$ is raised to the magnitude of 10^3 pm/V. It is worth mentioning that there are two approaches for the coupling of plasmonic nanostructures and MQWs. One approach is loading the metallic meta-atoms upon the MQW substrate,[14,16] and the other is constructing hybrid meta-atoms of metal and MQW.[21,35] To ensure good effect of beam shaping, the coupling between neighboring elements should be weak.[37] The real-space separation of MQW is beneficial for this condition, hence, we choose the second strategy. The proposed meta-atom is shown in Figure 2b. The electric field enhancement effect of highly confined plasmonic resonances enables efficient coupling with normal components of intersubband transitions, which brings a strong improvement for light−matter interaction and boosts the nonlinear processes to a greater extent. The comparison of the second-order susceptibility for

https://doi.org/10.1021/acsphotonics.1c00330
ACS Photonics 2021, 8, 1896−1902

the hybrid gold-MQW nanostructures and other materials mentioned above is given in Table 1.

Table 1. Second-Order Susceptibility for the Hybrid Gold-MQW Nanostructures and Other Materials Commonly Used in Photonics

material	$\chi^{(2)}_{eff}$, pm/V	λ_ω, nm	ref
hybrid gold-MQW nanostructures	$>10^3$	920	16
plasmonic nanostructures	10^1~10^2	1100~1500	11, 31
AlGaAs	100	1554	33, 34
$LiNbO_3$	27 (d_{33})	1064	32, 38
$KTiOPO_4$	10.7 (d_{33})	1064	38
β-BaB_2O_4	2.3 (d_{22})	1064	38

To illustrate the modulation effect of our proposed nonlinear wavy metasurfaces, several one-dimensional cases are calculated and exhibited. As is discussed above, the simplest case is the superposition of two equally weighted exponential terms with ±1 order. The expression is $\chi^{(2)}(x) = \chi_{eff}\cdot\sin(2\pi x/\Lambda + \theta) = \chi_{eff}\cdot\sum_{\pm1}(m/2i)\exp[im(2\pi x/\Lambda + \theta)]$, and here Λ is the modulation periodicity of meta-atoms. In this situation, as the whole distribution of $\chi^{(2)}$ is in the field of real number, the orientation of meta-atoms is either 0 or π. The local absolute value of $\chi^{(2)}$ related to the geometry of meta-atoms should be determined by eqs 3 and 4. The width and height of meta-atoms are chosen to be 80 and 30 nm, respectively. As the most representative geometry factor,[11] the ratio L_a/L_b is calculated along the x axis, while the total effective length $L_{eff} = 2L_a + L_b$ is invariant with the value 800 nm. The results are shown in Figure 3a together with the orientation as a discretized function. The corresponding Fourier spectrum is shown in Figure 3b. The conversion efficiency of this process can be evaluated based on eq 1. The $\chi^{(2)}_{eff}$ is set as ~10^3 pm/V, and the effective thickness of the metasurface is 100 nm. The wavelength of the pump light is chosen to be 920 nm, and the power is 1 W. The input polarization should be parallel to the base of SRRs,[11,39] and the polarization of the second harmonic field nearly lies in the orthogonal direction.[39,40] As the transmission-type metasurfaces are proposed, and the normally incident light is supposed, we mainly focus on the diffracted field, which is distinct from the reflection-type systems.[14,21,35] The corresponding general conversion efficiency of second harmonic generation is evaluated to reach the magnitude of 10^{-5}, which verifies the enhancement effect of MQW.

For more complex cases, we first consider $\chi^{(2)}(x) = 0.668\chi_{eff}\cdot[0.5\cdot\sin(2\pi x/\Lambda + \theta) + \sin(4\pi x/\Lambda + 3\theta)] = 0.668\chi_{eff}\cdot\sum_{\pm1}\{(m/4i)\exp[im(2\pi x/\Lambda + \theta)] + (m/2i)\exp[im(4\pi x/\Lambda + 3\theta)]\}$. The corresponding ratio L_a/L_b along the x axis is plotted in Figure 3c, and the Fourier spectrum is given in Figure 3d. In this case, the weight of ±1 order is smaller, and the multiplying power of OAM is not equal to that of the spatial frequency. These characters are distinct from conventional binary $\chi^{(2)}$ systems. Moreover, another rule in binary systems is that the attached OAM value increases with the diffraction order, but this can be broken in our proposed framework through suitable design. An available case is $\chi^{(2)}(x) = 0.471\chi_{eff}\cdot[\sin(2\pi x/\Lambda + \theta) + \sin(4\pi x/\Lambda + 3\theta) + 0.5\cdot\sin(6\pi x/\Lambda + 2\theta)] = 0.471\chi_{eff}\cdot\sum_{\pm1}\{(m/2i)\exp[im(2\pi x/\Lambda + \theta)] + (m/2i)\exp[im(4\pi x/\Lambda + 3\theta)] + (m/4i)\exp[im(6\pi x/\Lambda + 2\theta)]\}$. The spiral phase θ, 2θ, and 3θ for producing OAM are attached to different phase gradients along the x direction, decided by $2\pi x/\Lambda$, $6\pi x/\Lambda$, and $4\pi x/\Lambda$, respectively. A phase gradient brings a reciprocal vector, which

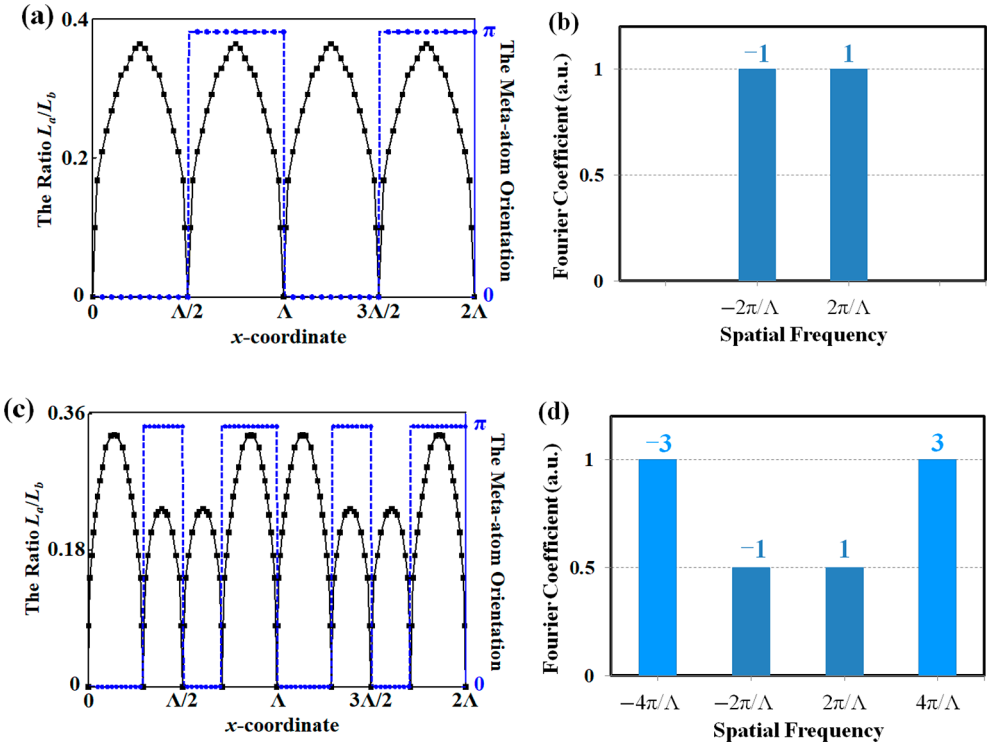

Figure 3. Ratio L_a/L_b along the x axis for (a) $\chi^{(2)}(x) = \chi_{eff}\cdot\sin(2\pi x/\Lambda + \theta) = \chi_{eff}\cdot\sum_{\pm1}(m/2i)\exp[im(2\pi x/\Lambda + \theta)]$ and (c) $\chi^{(2)}(x) = 0.668\chi_{eff}\cdot[0.5\cdot\sin(2\pi x/\Lambda + \theta) + \sin(4\pi x/\Lambda + 3\theta)] = 0.668\chi_{eff}\cdot\sum_{\pm1}\{(m/4i)\exp[im(2\pi x/\Lambda + \theta)] + (m/2i)\exp[im(4\pi x/\Lambda + 3\theta)]\}$, and the correspond Fourier spectrum (b) and (d), respectively.

https://doi.org/10.1021/acsphotonics.1c00330
ACS Photonics 2021, 8, 1896−1902

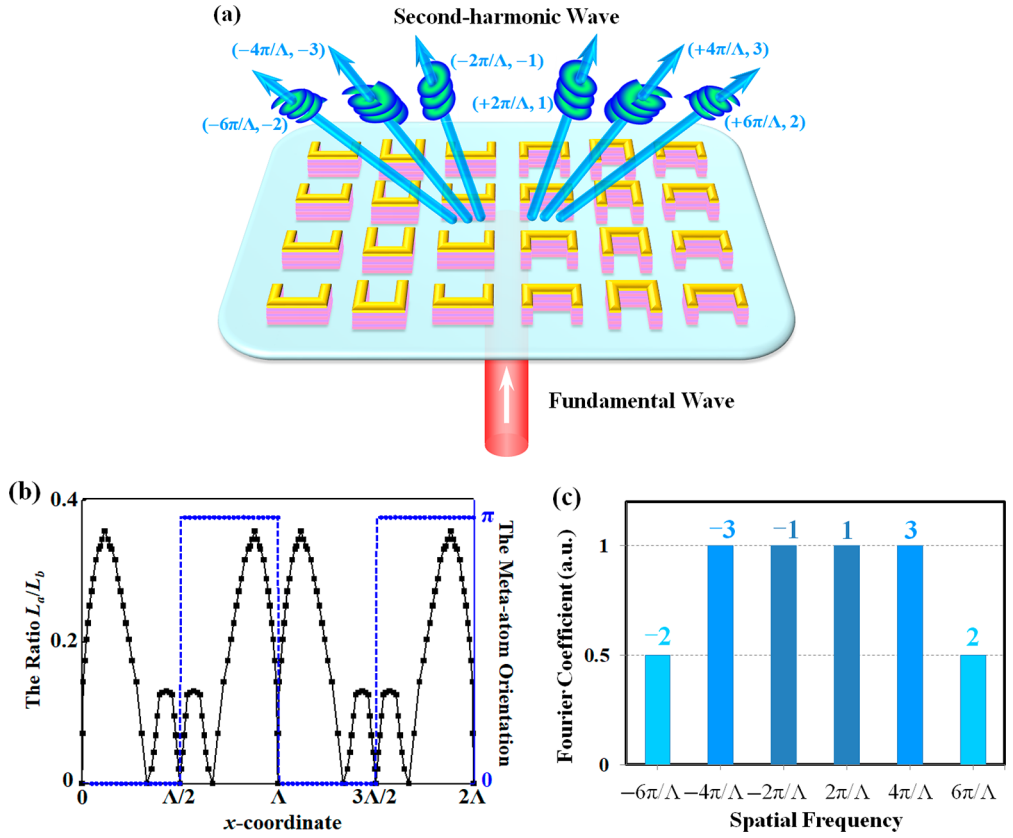

Figure 4. (a) Schematic of the diffraction at the metasurface with $\chi^{(2)}(x) = 0.471\chi_{eff}[\sin(2\pi x/\Lambda + \theta) + \sin(4\pi x/\Lambda + 3\theta) + 0.5\cdot\sin(6\pi x/\Lambda + 2\theta)] = 0.471\chi_{eff}\sum_{\pm 1}\{(m/2i)\exp[im(2\pi x/\Lambda + \theta)] + (m/2i)\exp[im(4\pi x/\Lambda + 3\theta)] + (m/4i)\exp[im(6\pi x/\Lambda + 2\theta)]\}$. The reciprocal vector and topological charge for each diffraction order are marked in the brackets. The corresponding L_a/L_b along the x axis and Fourier spectrum are shown in (b) and (c). It can be seen that the OAM states with topological charge ±3 are assigned to ±2 order corresponding to the terms with $4\pi x/\Lambda$, while those possessing OAM of $\pm 2\hbar$ are deflected into ±3 order arising from the terms with $6\pi x/\Lambda$. This breaks the conventional sense in binary $\chi^{(2)}$ systems that the attached OAM value increases with the diffraction order.

determines the diffraction direction denoted by the corresponding diffraction order. Therefore, it could be seen that the OAM states with topological charge ±3 are assigned to ±2 order, corresponding to the terms with $4\pi x/\Lambda$, while those possessing OAM of $\pm 2\hbar$ are deflected into ±3 order arising from the terms with $6\pi x/\Lambda$. A schematic of the diffraction at the metasurface for this case is shown in Figure 4a. The corresponding L_a/L_b along the x axis and Fourier spectrum are shown in Figure 4b and c, respectively. In binary systems, though the multiple periodic modulation of $\chi^{(2)}$ can change the conventional situation, the diffraction output is multi-ordered whose effects are far from ideal.

Precise local tailoring of $\chi^{(2)}$ based on nonlinear wavy metasurfaces can facilitate second harmonic beam shaping that is not available with conventional materials, which paves the way for various new possibilities in photonic applications. Besides the one-dimensional cases discussed above, the system is possible to be directly extended to modulate two-dimensional OAM arrays. Furthermore, the wavy metasurfaces could also be designed for realizing quasi-periodic and compound periodic distribution of $\chi^{(2)}$, which is available for finer and more complex manipulation of the spatial degree of freedom to demonstrate fantastic phenomena like fractal and super-diffraction.[41,42] Another potential exploration direction is tailoring the special spatial modes of a photon such as the Hermite-Laguerre-Gaussian mode,[43] the value of the proposed framework in optical information applications can be further exploited.

In conclusion, we develop a design framework of nonlinear wavy metasurfaces for generating and steering second-harmonic beams. The metasurfaces consist of hybrid meta-atoms of metal and MQW. The MQWs possess giant second-order nonlinearity, which ease the plight of low conversion efficiency faced by the metasurface based on pure metallic meta-atoms. Through introducing topological defects into the spatial distribution of $\chi^{(2)}$, OAM states can be obtained for the diffraction output. Choosing appropriate sinusoids with predefined coefficients for superposition, the corresponding Fourier spectrum is able to be engineered as desired, which is rarely demonstrated in previously proposed nonlinear metasurfaces. A series of distinct characters emerge comparing to conventional binary $\chi^{(2)}$ systems. Several one-dimensional cases are calculated to show the detailed effects. Such a platform sheds new light on future applications of quantum nanophotonics and topological photonics.

METHODS

Second-Order Nonlinear Response of Metasurface. According to the Lorentz reciprocity theorem with the assumption that saturation effects are neglected, the product of current density J at one position and electric field E at another position is unchanged when these two positions are switched, which is expressed as

https://doi.org/10.1021/acsphotonics.1c00330
ACS Photonics 2021, 8, 1896−1902

$$\int_V J_1 \cdot E_2 \, dV = \int_V J_2 \cdot E_1 \, dV \tag{6}$$

In our situation, the equivalent current density at second harmonic frequency excited by the induced fundamental field $E_n(\omega)$ can be given as

$$J(2\omega; \vec{r}) = 2i\omega P(2\omega; \vec{r}) = 2i\omega\varepsilon_0\chi^{(2)}E_n(\omega; \vec{r})^2 \tag{7}$$

Using the reciprocity relation and assuming a current dipole J' placing at the observation position, the radiated second harmonic field is derived to be

$$E_{SH} \propto i\omega\chi^{(2)}\left[\int E_n(2\omega)E_n(\omega)^2 \, dV\right] \tag{8}$$

After normalizing by the incident fields, this formula can be generalized to arbitrary polarization of induced fundamental and second harmonic modes, thus, eq 4 is obtained.

AUTHOR INFORMATION

Corresponding Authors

Yu-shen Liu − *School of Electronic and Information Engineering, Changshu Institute of Technology, Suzhou 215000, China;* orcid.org/0000-0002-5848-7670; Email: ysliu@cslg.edu.cn

Yan-qing Lu − *National Laboratory of Solid State Microstructures, College of Engineering and Applied Sciences, Nanjing University, Nanjing 210093, China;* orcid.org/0000-0001-6151-8557; Email: yqlu@nju.edu.cn

Authors

Yang Ming − *School of Electronic and Information Engineering, Changshu Institute of Technology, Suzhou 215000, China; National Laboratory of Solid State Microstructures, College of Engineering and Applied Sciences, Nanjing University, Nanjing 210093, China; SUPA, Institute of Photonics and Quantum Sciences, School of Engineering and Physical Sciences, Heriot-Watt University, Edinburgh EH14 4AS, United Kingdom;* orcid.org/0000-0002-4237-1083

Wang Zhang − *National Laboratory of Solid State Microstructures, College of Engineering and Applied Sciences, Nanjing University, Nanjing 210093, China*

Jie Tang − *School of Sciences, Nantong University, Nantong 226019, China*

Xifeng Yang − *School of Electronic and Information Engineering, Changshu Institute of Technology, Suzhou 215000, China*

Complete contact information is available at: https://pubs.acs.org/10.1021/acsphotonics.1c00330

Notes

The authors declare no competing financial interest.

ACKNOWLEDGMENTS

This work was supported by the National Key Research and Development Program of China (Grant No. 2017YFA0303700), the National Natural Science Foundation of China (NSFC) (Grant Nos. 11704182 and 62074019), and the Outstanding Scientific and Technological Innovation Team of Jiangsu Province (Grant No. 2017-27). Y.M. acknowledges the sponsorship of Jiangsu Government Scholarship for Overseas Studies, 2019.

REFERENCES

(1) Chen, H. T.; Taylor, A. J.; Yu, N. A Review of Metasurfaces: Physics and Applications. *Rep. Prog. Phys.* **2016**, *79* (7), 076401.

(2) Song, X.; Huang, L. L.; Sun, L.; Zhang, X.; Zhao, R.; Li, X.; Wang, J.; Bai, B.; Wang, Y. Near-Field Plasmonic Beam Engineering with Complex Amplitude Modulation Based on Metasurface. *Appl. Phys. Lett.* **2018**, *112* (7), 073104.

(3) Gennaro, S. D.; Li, Y.; Maier, S. A.; Oulton, R. F. Nonlinear Pancharatnam-Berry Phase Metasurfaces beyond the Dipole Approximation. *ACS Photonics* **2019**, *6* (9), 2335−2341.

(4) Kamali, S. M.; Arbabi, E.; Arbabi, A.; Faraon, A. A Review of Dielectric Optical Metasurfaces for Wavefront Control. *Nanophotonics* **2018**, *7* (6), 1041−1068.

(5) Yan, L.; Zhu, W.; Karim, M. F.; Cai, H.; Gu, A. Y.; Shen, Z.; Chong, P. H. J.; Tsai, D. P.; Kwong, D. L.; Qiu, C. W.; Liu, A. Q. Arbitrary and Independent Polarization Control In Situ via a Single Metasurface. *Adv. Opt. Mater.* **2018**, *6* (21), 1800728.

(6) Intaravanne, Y.; Chen, X. Z. Recent Advances in Optical Metasurfaces for Polarization Detection and Engineered Polarization Profiles. *Nanophotonics* **2020**, *9* (5), 1003−1014.

(7) Li, S. Q.; Xu, X.; Veetil, R. M.; Valuckas, V.; Paniagua-Domínguez, R.; Kuznetsov, A. I. Phase-only Transmissive Spatial Light Modulator Based on Tunable Dielectric Metasurface. *Science* **2019**, *364* (6445), 1087−1090.

(8) Zhang, X.; Xu, N.; Qu, K.; Tian, Z.; Singh, R.; Han, J.; Agarwal, G. S.; Zhang, W. Electromagnetically Induced Absorption in a Three-Resonator Metasurface System. *Sci. Rep.* **2015**, *5*, 10737.

(9) O'Brien, K.; Suchowski, H.; Rho, J.; Salandrino, A.; Kante, B.; Yin, X.; Zhang, X. Predicting Nonlinear Properties of Metamaterials from the Linear Response. *Nat. Mater.* **2015**, *14* (4), 379−383.

(10) Li, G. X.; Chen, S. M.; Pholchai, N.; Reineke, B.; Wong, P. W. H.; Pun, E. Y. B.; Cheah, K. W.; Zentgraf, T.; Zhang, S. Continuous Control of the Nonlinearity Phase for Harmonic Generations. *Nat. Mater.* **2015**, *14* (6), 607−612.

(11) Keren-Zur, S.; Avayu, O.; Michaeli, L.; Ellenbogen, T. Nonlinear Beam Shaping with Plasmonic Metasurfaces. *ACS Photonics* **2016**, *3* (1), 117−123.

(12) Schlickriede, C.; Waterman, N.; Reineke, B.; Georgi, P.; Li, G. X.; Zhang, S.; Zentgraf, T. Imaging through Nonlinear Metalens Using Second Harmonic Generation. *Adv. Mater.* **2018**, *30* (8), 1703843.

(13) Ming, Y.; Zhang, W.; Tang, J.; Liu, Y.; Xia, Z.; Liu, Y. S.; Lu, Y. Q. Photonic Entanglement Based on Nonlinear Metamaterials. *Laser Photonics Rev.* **2020**, *14* (5), 1900146.

(14) Lee, J.; Tymchenko, M.; Argyropoulos, C.; Chen, P. Y.; Lu, F.; Demmerle, F.; Boehm, G.; Amann, M. C.; Alù, A.; Belkin, M. A. Giant Nonlinear Response from Plasmonic Metasurfaces Coupled to Intersubband Transitions. *Nature* **2014**, *511* (7507), 65−69.

(15) Shen, K. C.; Huang, Y. T.; Chung, T. L.; Tseng, M. L.; Tsai, W. Y.; Sun, G.; Tsai, D. P. Giant Efficiency of Visible Second-Harmonic Light by an All-Dielectric Multiple-Quantum- Well Metasurface. *Phys. Rev. Appl.* **2019**, *12* (6), 064056.

(16) Qian, H.; Li, S.; Chen, C. F.; Hsu, S. W.; Bopp, S. E.; Ma, Q.; Tao, A. R.; Liu, Z. W. Large Optical Nonlinearity Enabled by Coupled Metallic Quantum Wells. *Light: Sci. Appl.* **2019**, *8*, 13.

(17) Lassaline, N.; Brechbühler, R.; Vonk, S. J. W.; Ridderbeek, K.; Spieser, M.; Bisig, S.; Le Feber, B.; Rabouw, F. T.; Norris, D. J. Optical Fourier Surfaces. *Nature* **2020**, *582* (7813), 506−510.

(18) Bloch, N. V.; Shemer, K.; Shapira, A.; Shiloh, R.; Juwiler, I.; Arie, A. Twisting Light by Nonlinear Photonic Crystals. *Phys. Rev. Lett.* **2012**, *108* (23), 233902.

(19) Ming, Y.; Tang, J.; Chen, Z. X.; Xu, F.; Zhang, L. J.; Lu, Y. Q. Generation of N00N State With Orbital Angular Momentum in a Twisted Nonlinear Photonic Crystal. *IEEE J. Sel. Top. Quantum Electron.* **2015**, *21* (3), 225.

(20) Porat, G.; Silberberg, Y.; Arie, A.; Suchowski, H. Two Photon Frequency Conversion. *Opt. Express* **2012**, *20* (4), 3613−3619.

(21) Kim, D.; Chung, H.; Yu, J.; Hwang, I.; Park, S.; Demmerle, F.; Boehm, G.; Amann, M. C.; Belkin, M. A.; Jung, J. Y.; Lee, J. Spin-

Controlled Nonlinear Harmonic Generations from Plasmonic Metasurfaces Coupled to Intersubband Transitions. *Adv. Opt. Mater.* **2020**, *8* (8), 2000004.
(22) Wang, J.; Yang, J. Y.; Fazal, I. M.; Ahmed, N.; Yan, Y.; Huang, H.; Ren, Y.; Yue, Y.; Dolinar, S.; Tur, M.; Willner, A. E. Terabit Free-Space Data Transmission Employing Orbital Angular Momentum Multiplexing. *Nat. Photonics* **2012**, *6* (7), 488−496.
(23) Ming, Y.; Chen, P.; Ji, W.; Wei, B. Y.; Lee, C. H.; Lin, T. H.; Hu, W.; Lu, Y. Q. Tailoring the Photon Spin via Light−Matter Interaction in Liquid-Crystal-Based Twisting Structures. *npj Quantum Mater.* **2017**, *2*, 6.
(24) Ni, J. C.; Liu, S. L.; Wu, D.; Lao, Z. X.; Wang, Z. Y.; Huang, K.; Ji, S. Y.; Li, J. W.; Huang, Z. X.; Xiong, Q. H.; Hu, Y. L.; Chu, J. R.; Qiu, C. W. Gigantic Vortical Differential Scattering as a Monochromatic Probe for Multiscale Chiral Structures. *Proc. Natl. Acad. Sci. U. S. A.* **2021**, *118* (2), e2020055118.
(25) Ni, J. C.; Liu, S. L.; Hu, G. W.; Hu, Y. L.; Lao, Z. X.; Li, J. W.; Zhang, Q.; Wu, D.; Dong, S. H.; Chu, J. R.; Qiu, C. W. Giant Helical Dichroism of Single Chiral Nanostructures with Photonic Orbital Angular Momentum. *ACS Nano* **2021**, *15* (2), 2893−2900.
(26) Wang, B.; Liu, W. Z.; Zhao, M. X.; Wang, J. J.; Zhang, Y. W.; Chen, A.; Guan, F.; Liu, X. H.; Shi, L.; Zi, J. Generating Optical Vortex Beams by Momentum-Space Polarization Vortices Centred at Bound States in the Continuum. *Nat. Photonics* **2020**, *14* (10), 623−628.
(27) Li, H.; Liu, H. G.; Chen, X. F. Nonlinear Vortex Beam Array Generation by Spatially Modulated Fundamental Wave. *Opt. Express* **2017**, *25* (23), 28668−28673.
(28) Boyd, R. W. *Nonlinear Optics*, 3rd ed.; Elsevier: New York, 2008.
(29) Allen, L.; Beijersbergen, M. W.; Spreeuw, R. J. C.; Woerdman, J. P. *Phys. Rev. A: At., Mol., Opt. Phys.* **1992**, *45* (11), 8185−8189.
(30) Zhang, S.; Huo, P.; Zhu, W.; Zhang, C.; Chen, P.; Liu, M.; Chen, L.; Lezec, H. J.; Agrawal, A.; Lu, Y. Q.; Xu, T. Broadband Detection of Multiple Spin and Orbital Angular Momenta via Dielectric Metasurface. *Laser Photonics Rev.* **2020**, *14* (9), 2000062.
(31) Segal, N.; Keren-Zur, S.; Hendler, N.; Ellenbogen, T. Controlling Light with Metamaterial-Based Nonlinear Photonic Crystals. *Nat. Photonics* **2015**, *9* (3), 180−184.
(32) Ming, Y.; Wu, Z. J.; Cui, G. X.; Tan, A. H.; Xu, F.; Lu, Y. Q. Integrated Source of Tunable Nonmaximally Mode-Entangled Photons in a Domain Engineered Lithium Niobate Waveguide. *Appl. Phys. Lett.* **2014**, *104* (17), 171110.
(33) Sain, B.; Meier, C.; Zentgraf, T. Nonlinear Optics in All-Dielectric Nanoantennas and Metasurfaces: a Review. *Adv. Photonics* **2019**, *1* (2), 024002.
(34) Gili, V. F.; Carletti, L.; Locatelli, A.; Rocco, D.; Finazzi, M.; Ghirardini, L.; Favero, I.; Gomez, C.; Lemaître, A.; Celebrano, M.; De Angelis, C.; Leo, G. Monolithic AlGaAs Second-Harmonic Nanoantennas. *Opt. Express* **2016**, *24* (14), 15965−15971.
(35) Lee, J.; Nookala, N.; Gomez-Diaz, J. S.; Tymchenko, M.; Demmerle, F.; Boehm, G.; Amann, M. C.; Alù, A.; Belkin, M. A. Ultrathin Second-Harmonic Metasurfaces with Record-High Nonlinear Optical Response. *Adv. Opt. Mater.* **2016**, *4* (5), 664−670.
(36) Frigerio, J.; Ballabio, A.; Ortolani, M.; Virgilio, M. Modeling of Second Harmonic Generation in Hole-Doped Silicon Germanium Quantum Wells for Mid-Infrared Sensing. *Opt. Express* **2018**, *26* (24), 31861−31872.
(37) Tymchenko, M.; Gomez-Diaz, J. S.; Lee, J.; Nookala, N.; Belkin, M. A.; Alù, A. Gradient Nonlinear Pancharatnam-Berry Metasurfaces. *Phys. Rev. Lett.* **2015**, *115* (20), 207403.
(38) Dmitriev, V. G.; Gurzadyan, G. G.; Nikogosyan, D. N. *Handbook of Nonlinear Optical Crystals*, 3rd ed.; Springer: Berlin, 1999.
(39) Klein, M. W.; Enkrich, C.; Wegener, M.; Linden, S. Second-Harmonic Generation from Magnetic Metamaterials. *Science* **2006**, *313* (5786), 502−504.
(40) Ciracì, C.; Poutrina, E.; Scalora, M.; Smith, D. R. Origin of Second-Harmonic Generation Enhancement in Optical Split-Ring Resonators. *Phys. Rev. B: Condens. Matter Mater. Phys.* **2012**, *85* (20), 201403.
(41) Zhang, W.; Tang, J.; Chen, P.; Cui, G. X.; Ming, Y.; Hu, W.; Lu, Y. Q. Evolution of Orbital Angular Momentum in a Soft Quasi-Periodic Structure with Topological Defects. *Opt. Express* **2019**, *27* (15), 21667−21676.
(42) Zhang, Y.; Huang, C. P.; Chang, H. C. Super Diffraction in a Single-Layer Metasurface. *J. Lightwave Technol.* **2016**, *34* (14), 3312−3316.
(43) Tang, J.; Ming, Y.; Chen, Z. X.; Hu, W.; Xu, F.; Lu, Y. Q. Entanglement of Photons with Complex Spatial Structure in Hermite-Laguerre-Gaussian Modes. *Phys. Rev. A: At., Mol., Opt. Phys.* **2016**, *94* (1), 012313.

https://doi.org/10.1021/acsphotonics.1c00330
ACS Photonics 2021, 8, 1896−1902